International Research Journal of Engineering and Technology (IRJET) e-ISSN: 2395-0056
Volume: 08 Issue: 07 | July 2021 www.irjet.net p-ISSN: 2395-0072

Numerical Modelling and Performance Analysis of Flat Slab Subjected to Fire Condition

Kamlesh Bhanarkar[1], Prof. Dr. Nina Dhamge[2], Prof. Vinayak Vaidya[3]

[1]Student M.Tech. Structural Engg. B.E. Civil Engg. Nagpur Maharashtra India
[2]Ph. D. Professor in Dept. of Civil Engg, KDKCE, Nagpur Maharashtra India
[3]Example: Ph. D. Professor in Dept. of Civil Engg, KDKCE, Nagpur Maharashtra India

---

Abstract - *In this study, a finite element model was developed using Abaqus to analyse the impact of elevated temperature on flat slab-column assembly. The slab-column model gives temperature distributions in the flat slab for the material properties and boundary conditions feed in the model. By using finite element analysis, the entire reinforced slab column assembly meshed into small segments called elements. The elements possess the physical properties of their corresponding materials. Each element in the model was bounded by nodal points. Boundary conditions were included on the appropriate nodes in the model. The analysis was conducted for different boundaries such as pin-pin, and fixed on both ends. The results obtained from the analyses of the given model are dependent on time, including thermal distribution, deflection, stresses and strains. From the results, the magnitude and location of maximum stress, strain and displacement generated in the model for different boundary conditions were determined with the analysis. Transient Heat Analysis were compared with the results provided in the referred literature studies. It was found that the results from the transient heat transfer analysis are very similar to the temperature distribution determined in Weerasinghe et al and Smith et al. This paper presents the comparison of finite element analysis of experimental works related to flat slab-column assembly. The study aims to demonstrate the effectiveness of FEM in analysing the complex behaviour of flat slab-column assembly with considering the different reinforcement ratios, geometry, load and support conditions of flat slab.*

Key Words: Flat slab. Slab column assembly, Punching shear, Finite element modelling, Abaqus, ISO 384 fire curve.

1.INTRODUCTION

Flat slab design in contemporary buildings is being preferred due to its various advantages like reduced floor height, simple formwork, easing installation of services and succinctly cost-effectiveness. Although the flat slab design has benefits, the flat slab structures are considered vulnerable to punching shear. To overcome the punching shear failure of the flat slab at the slab-column junction, several modifications have been carried out such as providing column cap, drop panel and shear reinforcement at slab-column junction. However, the junction area of flat slab-column remains a critical section for the punching shear effect. This punching shear effect gets exaggerated in the elevated temperature condition during fire. In last one and half decade, handful experimental studies have been carried out to understand the behaviour of critical section of flat slab-column junction in higher temperature. Only a limited studies have been carried out to analyse the effect of elevated temperature in flat slab by finite element modelling.

Large thermal gradients are observed within concrete, especially in case of deep specimens. Large thermal gradients in concrete causes differential expansion, and this leads to the convergence problem in finite element modelling. It can also damage within the material when the concrete member is subjected to fire. Concrete and steel have different coefficient of thermal expansion. When the reinforced concrete gets heated, due to the different thermal expansion of the two materials the reinforced concrete undergoes large plastic deformation around the reinforcement embedded in it. This also have to be considered as a reason for damage in concrete subjected to fire. This, combinedly with the change in mechanical properties of both the materials at higher temperatures, complicates analysis which have been modelled to replicate these actual experiments. The aim of this study is to compare the results of the FEM modelling and the results obtained from the experimental work.

It is very challenging to develop a finite element (FE) model that precisely represents the behaviour of a reinforced concrete structure at high temperature.

To get the results which resembles the results obtained from the experimental work requires a complex approach of modelling and data feed in to the model such as the Concrete damaged plasticity (CDP) in Abaqus (Dassault Systèmes, 2012). The response of the structural model, depends upon the material properties fed in to the model and solution parameters. In the studies conducted by the researchers eg. (Al Hamd et al., 2018; Weerasinghe et al., 2018), the detailed material properties which required for CDP have not been reported.

2. THE REFERENCE FLAT SLAB FROM LITERATURE

This paper has referred two studies in which the flat slab was studies under the effect of fire. In this study the

flat slab in literature has been modelled in Abaqus and has been exposed to the similar fire conditions to evaluate and compare the results obtained in FE analysis and experimental work. The two literature and samples considered for the current studies are as follows:

A. Weerasinghe et al. 2020

B. H.K.M. Smith 2016

The characteristics of flat slab model in study conducted by Weerasiinghe et al. 2020, Slab size was 3.78 m × 4.75 m having a thickness of 180 mm and have a column stub of 0.25 m × 0.25 m x 0.4 m connected at the centre. The concrete cover was 29 mm which corresponds to an axis distance of 35 mm. The thickness was taken as 180 mm as it was needed to find out the fire-resistant duration of a slab below 200 mm thickness as specified by EC2 part 1–2 [5] for 90 min and Fig shows the size and reinforcement detailing of the slab specimen.

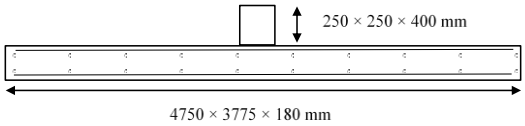

Fig. 2.1 Cross section of reinforced flat slab with column

For the flexural reinforcement at the bottom, 12 mm diameter deformed bars were positioned in two orthogonal directions with a spacing of 100 mm which corresponds to a reinforcement ratio(ρ) of 0.9%. A 200 mm × 200 mm spaced square rebar mesh having 10 mm diameter bars were used as top reinforcement (ρ = 0.3%). 8 bars of 20 mm diameter bars were positioned in the column along with stirrups of 6 mm diameter along the height of the column with 80 mm spacing. However, for the simplicity of the model, and analysis, we have not considered the column reinforcement embedded. Since the column reinforcement dies not affect the flexural behavior of flat slab and only purpose to carry stresses generated in it. Instead, we have shortened the height of column so as to pass the applied load directly on the slab without any resistance by the column itself.

The material properties and test conditions were provided as follows:

Compressive strength (7 days) = 26 MPa

Compressive strength (28 days) = 39 MPa

Tensile strength (28 days) = 3.7 MPa

Young's modulus (28 days) = 28600 MPa

Poisson's ratio (28 days) = 0.21

Axial Load = 225 kN–275 kN

Fire temperature and time = ISO 834 fire curve, heating for 3.5 h and cooling down up to 12 h.

Support conditions to slab: Partially restrained as shown in Fig. 2.2

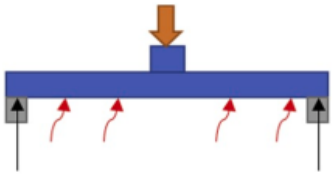

Fig. 2.2. Support, fire source and loading condition in flat slab

In the study carried out by H.K.M. Smith 2016, following slabs were tested with the different slab thickness and reinforcement ratios. The sizes of slab were common and are of 1400 × 1400 thickness 50,75,100 m with varying slab thickness as shown below:

The reinforcement bars were taken as 8 mm for main reinforcement and 6 mm for distribution bars. The column size was 120 × 120, 100 mm heigh.

- 50 mm thick, 0.8% reinforced
- 75 mm thick, 0.8% reinforced
- 100 mm thick, 0.8% reinforced
- 100 mm thick, 1.5% reinforced.

Compressive strength of concrete (28 days) = 51 MPa

Yield strength of steel = 550 MPa.

The mechanical properties were calculated based on the properties specified above.

Axial Load = 50 kN–250 kN

Fire temperature and time = Furnace specific. Max. temp. 510 ^{0}C, 2 h of heating and cooling down till 150 0C.

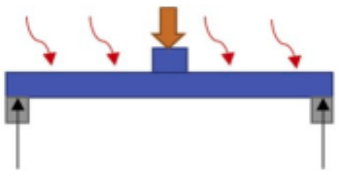

Fig. 2.3. Support, fire source and loading condition in flat slab

3. METHODOLOGY

The steps by step method adopted while modelling the flat slab assembly and structural performance of the same under elevated temperature conditions are as follows:

1. Modelling the 3-dimensional finite element model of the flat slab-column assembly used in the referred literature study. This involves the dimension of the concrete slab, column and reinforcements.
2. Appropriate modelling data calculation such as data of CDP to feed in the model. Selection of element and meshing, load applied and boundary conditions.
3. Applying the time dependent rise in temperature as given standard ISO 834 fire curve to the model on the portion as performed in the experimental work.
4. Running the first step of transient heat distribution analysis as a function of time.
5. Comparing the results obtained from the first step of heat distribution across the model and using the same file as an input for the second stage of sequentially coupled thermal analysis.
6. The temperature distribution across the slab from the first stage thermal analysis run is applied as nodal temperature in the model, while transverse loading as shown in experimental works is applied at the centrally located column.
7. Evaluating the deflection, total strains comprising mechanical and thermal strains and the associated stresses within slab cross sections, due to the applied transient thermal loading.

4. FINITE ELEMENT MODELLING

For the sequentially coupled thermal analysis which is two step analysis, two sub-models, namely, thermal and structural models, are needed. In first step, a thermal analysis is carried out on the thermal model, while in step two a structural model is fed with the first step thermal analysis results along with the loading and boundary conditions. The model has been discretized with different element in both steps, like for the thermal/heating step the concrete part has been discretized using 8-node linear heat transfer brick type (DC3D8), while for the reinforcement a 2-node heat transfer link (DC1D2) has been used. For the second step load analysis, the flat slab column model has been discretised by the eight-node linear brick 3D stress element (C3D8R), and the reinforcement has been discretized by using 2-node linear 3D truss element (T3D2) Fig. 3.1-3.4. In some numerical modelling studies, the concrete in model has been discretized using the same DC3D8 element, since this element type can be used for analysis of cracking and tensile stress in concrete (14). T3D2 elements are used to model one-dimensional reinforcing bars or rods that are assumed to deform by axial stretching only. They are pin jointed at their nodes; only translational displacements and the initial position vector at each node are used in the discretization. When the strains are large, the formulation is simplified by assuming that the trusses to be made of incompressible material. This approach has been used effectively to model reinforcement explicitly wherein nodes of reinforcement are coincident with corresponding nodes of concrete [14]. The interaction between concrete and reinforcement is achieved by using the embedded region constraint, i.e. defining reinforcement to be embedded in concrete.

While the beam elements are supposedly a more computationally efficient choice for both the structural and thermal models, prediction of an accurate temperature distribution within the member requires the use of three-dimensional elements. Moreover, similar modelling strategies have worked well for researchers in the past [12]. Finally, there is a possibility to extend such a model to include complex phenomenon like concrete spalling in future studies. A tie constraint is used to apply temperatures from concrete to reinforcing steel bars at that location Fig. 3.4.

The bottom and side face of the slab which are exposed to fire are used to simulate the surface effect of convection and radiation that occur from fire (ambient air) to the flat slab. As per EN 1991-1-2 [16], the value of convection fed to the model is recommended as 25 W/m2.C on fire exposed surface. For the un-exposed surfaces, the heat that may occur due to the radiation from the heated surface the a convective coefficient of 9 W/m2 C is used. The emissivity for radiative heat transfer at the exposed surfaces of the concrete member is taken as 0.8. Similar analysis parameters have yielded results with sufficient accuracy and efficiency in earlier studies [26].

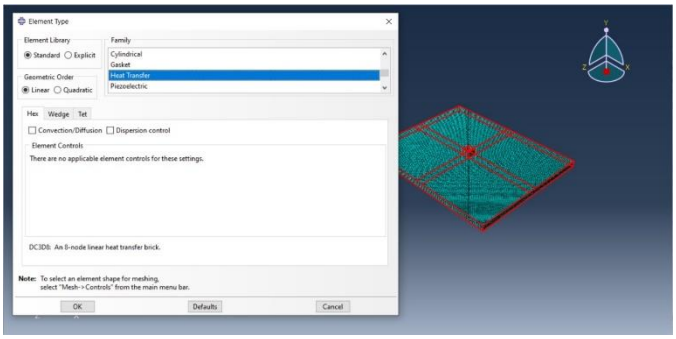

Fig. 3.1: Discretization using DC3D8 element

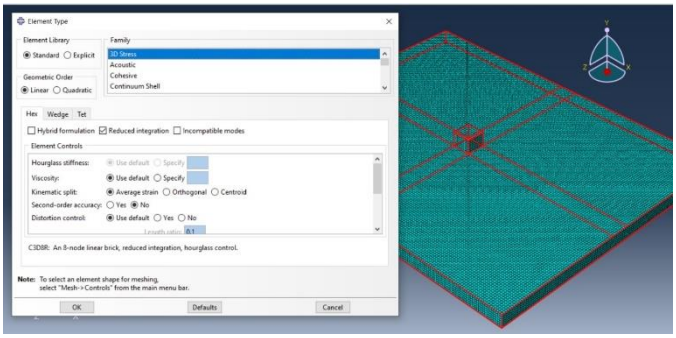

Fig. 3.2: Discretization using C3D8R element

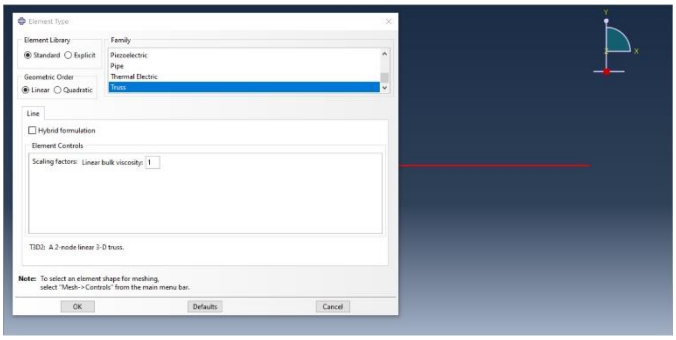

Fig. 3.3 Discretization using T3D2 element

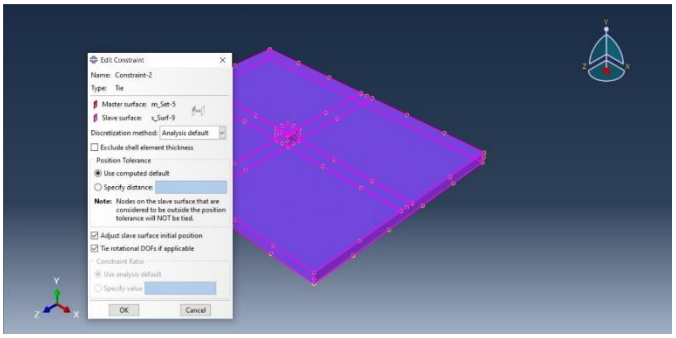

Fig. 3.4 Tie constraint in FEM model

3.1 Modelling Assumptions

Some assumptions have been considered for simplifying the modelling, data feed and analysis of the model:

1. The concrete strength of different mesh in the compression zone is different, but the strength in each mesh is regarded as a constant;
2. No bond-slip is assumed to occur between steel reinforcement and concrete implying that there is perfect bond and that the total strain in the reinforcement is equal to that in the concrete. [23]
3. The equivalent reduction coefficient of the concrete strength of the entire compression zone can be obtained by weighting the average of the cross-sectional compression zone area;
4. The heat loss due to moisture evaporation during the fire was not considered;

3.2 Thermal Properties of Material

To obtain temperature distribution of flat slab, heat transfer analysis was performed using Abaqus. The specific heat capacity, thermal conductivity, and density of the materials have been determined, which are the basis for the analysis. The parameters were selected based on formulae suggested in the study by Wang and He (2009).

The thermal conductivity of concrete λcT in (W/(m°C)), Specific Heat (J/Kg ^{0}C), Modulus of elasticity E in (MPa) and Poisson's Ratio.

$$\lambda cT = 2 - 0.24\left(\frac{T}{120}\right) + 0.012\left(\frac{T}{120}\right)^2 \quad (20^0C \le T \le 1200°C) \qquad 1$$

where T is the temperature, °C

The thermal conductivity of reinforcement steel λsT (W/ (m °C)) is

$$\lambda sT = 54 - 3.33 \times 10^{-2}T \quad (20^0C \le T \le 800°C)$$
$$\lambda sT = 27.3 \quad (800^0C \le T \le 1200°C) \qquad 2$$

The specific heat capacity of concrete CcT (J/(Kg °C)) is

$$C_{cT} = 900 + 80\left(\frac{T}{120}\right) - 4\left(\frac{T}{120}\right)^2 \quad (20^0C \le T \le 1200°C) \qquad 3$$

The specific heat capacity of reinforcement CsT (J/(Kg °C)) is

$$C_{sT} = 425 + 7.73 \times 10^{-1}T - 1.69 \times 10^{-3}T^2 + 2.22 \times 10^{-6}T^3 \quad (20^0C \le T \le 600°C) \qquad 4$$
$$C_{sT} = 666 + \frac{13002}{738 - T} \quad (600^0C \le T \le 735°C)$$
$$C_{sT} = 545 + \frac{17820}{T - 731} \quad (735^0C \le T \le 900°C)$$
$$C_{sT} = 650 \quad (900^0C \le T \le 1200°C)$$

3.3 Mechanical Properties of the Material.

A concrete damaged plasticity constitutive model [14] is generally used to model the complex behaviour of concrete in some studies, involving strong nonlinearity and different failure mechanisms under compression and tension (crushing or cracking). The stress–strain relation for concrete in tension is represented by a bilinear relationship which is elastic up to peak stress. The tensile strength of concrete at elevated temperatures is assumed to vary as per Eurocode 2 [16]

In Stage 2 of analysis, during heating phase, the temperature dependent thermal and mechanical properties of reinforcing steel and concrete are assumed to follow as that of Eurocode 2. Moreover, variation of the Poisson's ratio of concrete is assumed based on existing literature [15].

3.4 Standard Fire Curve

The heat transfer analysis was performed on the basis of a heating curve. Here the ISO-834 fire curve from the International Organization (ISO 1999) is adopted. The curve can be expressed as (Fu 2016b,2018)

$$T = T_0 + 345\log(8t + 1) \qquad 1$$

where t is the heating time (min); T_0 is the initial room temperature (°C, which is 20 °C here).

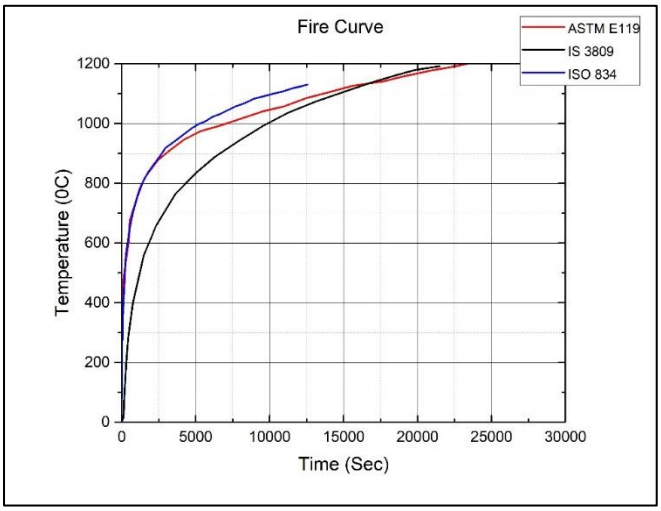

Fig. 3.5: Standard Fire Curve

5. OUTPUT RESULTS

Displacements, stresses and temperature fields are the primary output variables that are generated during different stages of analysis. In Stage 1 of analysis, the slab has been analysed for the distribution of temperature in slab and reinforcement. The resultant file was used to introduced in stage 2 of analysis where loading was introduced and propagated. At each time step, the output from the thermal analysis, namely nodal temperatures, is applied as a thermal body load on the structural elements (nodes) to evaluate the structural response of flat slab under fire exposure.

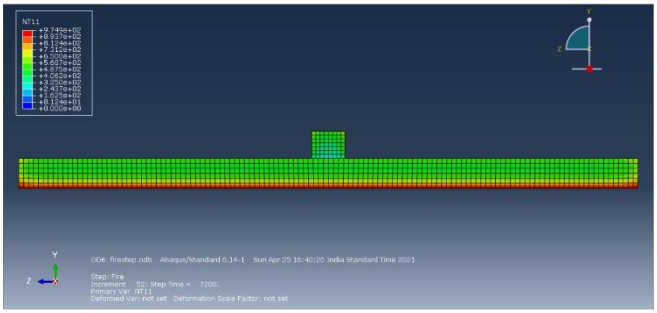

Fig. 4.1: Temperature distribution in FEM model

The results from the experimental work as discussed previously from the Weerasinghe et al and smith et al have been plotted. The results from FE modelling were plotted against the graphs/curves of experimental data. The comparative graph plotted suggest that the FE modelling results are in good agreement with the experimental work. The curves plotted indicates that there is slight variation in results from experimental and FE modelling, this may be due to the nonuniform heat distribution in experimental work during analysis. The results from the study have been discussed in detail below:

Comparison of the results from Weerasinghe et al. 2020 and current study of FE modelling and analysis:

1. The temperature rise on the surface of flat slab is rapid in early 4000 seconds and the rate of increase of temperature gradually gets slower. The phenomenon is similar to the fire curve which was used as an input. (Fig. 4.2)
2. The temperature distribution in middle part of the slab i.e., at 90 mm depth shows a linear increase in temperature instead of what was recorded on exposed surface. This shows that the concrete's thermal resistance has been come into play which resist the temperature rise but could not stop itself from the heating.
3. The comparative graph shows that, FE analysis results are in close agreement with the experimental results and hence proves the useability of FE modelling. The temperature rise in unexposed face is very less compared to the exposed and at centre. This might be due to the depth of slab and thermal resistance by the concrete.
4. Effect of temperature rise in reinforcement plays a very important role in deflection of flat slab and punching shear failure. The FE analysis results shows similar results in comparison with the experimental results.
5. Deflection of flat slab under the combined effect of loading and elevated temperature is an important measure of the study. The deflection calculated from FE modelling and analysis has been consistent with the experimental work within slight or very less deviation. The results from both the studies have been plotted in graph.

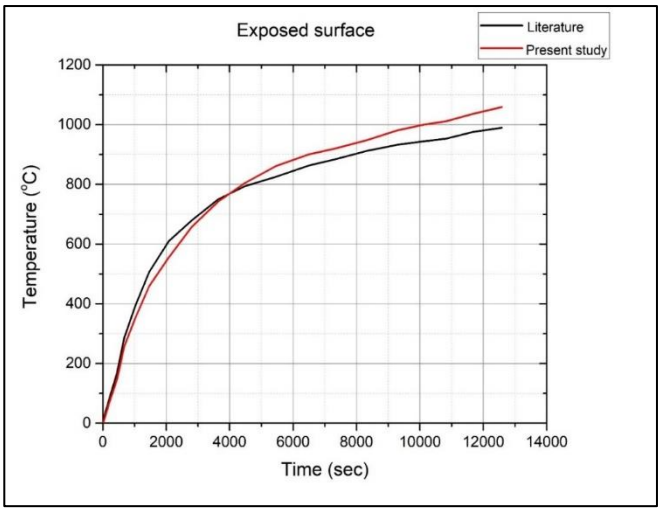

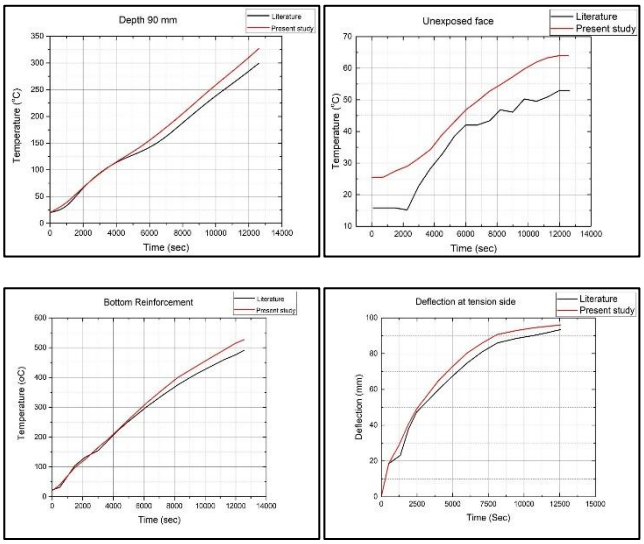

Fig. 4.2: Comparison of the results from Smith et al. 2015 and current study of FE modelling and analysis.

1. In present study, the model was created in Abaqus considering the geometry, material properties and support conditions as discussed in the referred literature. Comparative graphs of the results have been plotted are discussed below:
2. The resultant curves from FE analysis plotted shows close follow up of the experimental work for both the boundary conditions. However, it does not coincide with the curves for experimental work at the departing end.
3. The experimental results show that, the unrestrained slab fails at 250 seconds due to the load imposed on the slab. However, the FE analysis continues to analyse the slab till nearly 550 seconds.

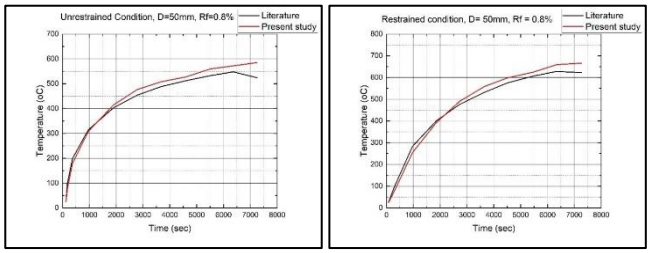

Fig.4.3: Comparison of results for the flat slab Depth = 50 mm, reinforcement ratio = 0.8% – restrained and unrestrained conditions:

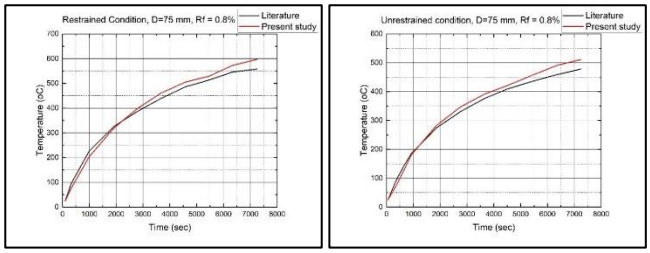

Fig. 4.4: Comparison of results for the flat slab Depth = 75 mm, reinforcement ratio = 0.8% – restrained and unrestrained conditions.

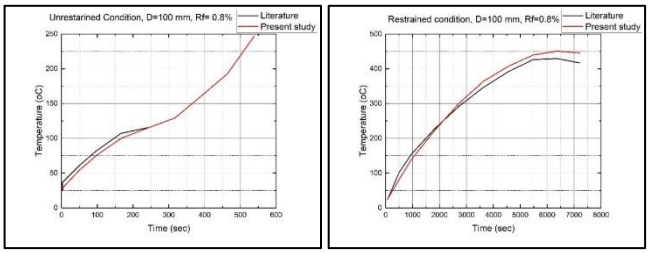

Fig.4.5: Comparison of results for the flat slab Depth = 100 mm, reinforcement ratio = 0.8% – restrained and unrestrained conditions.

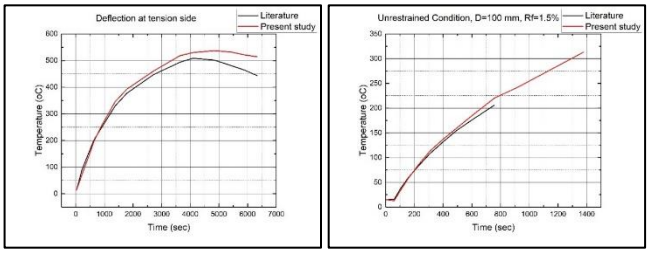

Fig.4.6: Comparison of results for the flat slab Depth = 100 mm, reinforcement ratio = 1.5% – restrained and unrestrained conditions.

6. CONCLUSIONS:

The heat transfer thermal analysis process available in Abaqus, sequentially modified coupled thermal analysis enabled us to produce a spectrum of time dependent results. Since the duration of both the analyses was varying from 1 hr to 3 hr, we were able to study the behaviour of reinforced cement concrete flat slab, comprising of normal strength concrete and high & medium strength mild steel reinforcing bars, subjected to a standard fire (ISO 834) and surface force of 275 KN, with different support conditions, for a period of 3hrs. Results were determined at the end of each minute throughout the analysis duration of 90 minutes.

1. The flat slab-column assembly can be accurately simulated using the sequential thermo-mechanical coupling model developed in Abaqus.
2. The fire exposure significantly weakened the flexural capacity and increase the deflection after a longer time of fire exposure.
3. The results obtained from the FEA shows a good agreement with the results obtained from experimental work for the stage 1 of heating. The results obtained for the deflection of slab, shows a little variation with the FEA results, this is because in the experimental work, the loading jack/ mechanism has very limited displacement range and when the slab exceeds this displacement range, the load transferred to the slab is decreases and hence the deflection beyond this displacement range of loading jack is shown less in experimental work, while in FEA analysis results, the deflection goes beyond the point shown in experimental results.
4. Among the influence factors, the boundary conditions, time of fire exposure, the ratio of longitudinal

reinforcement, and effective depth of slab all largely affected the flexural capacity of flat slab after fire exposure. The flexural capacity was enhanced with larger cover layer thickness or higher reinforcement ratio but reduced after longer time of fire exposure. The flexural capacity was severely weakened when the depth of slab is less and the load induced it increases.

7. REFERENCES

1. P. Olmati, J. Sagaseta, D. Cormie, A.E.K. Jones, "Simplified reliability analysis of punching in reinforced concrete flat slab buildings under accidental actions", Engineering Structures 130 83–98. (2017).
2. Y. Mirzaei, "Post punching behavior of reinforced slab-column connections", 7th fib PhD Symposium in Stuttgart, (2008).
3. D.T. Ngo, "Punching shear resistance of high-strength concrete slabs, Electronic journal of structural engineering", Vol. 1, pp. 52-59, (2001).
4. P. Bamonte, R. Felicetti, P.G. Gambarova,, "Punching Shear in Fire-damaged Reinforced Concrete Slabs", ACI Special Publication, SP265-16, pp. 345–366, (2009).
5. N.N. Brushlinsky, M. Ahrens, S.V. Sokolov, P. Wagner, "World Fire Statistics, Center of Fire Statistics of CTIF", International Association of Fire and Rescue Services, No.20, (2015).
6. C.E. Ospina, G. Birkle, Widianto," Databank of concentric punching shear tests of two-way concrete slabs without shear reinforcement at interior supports", ASCE Struct. Congr. 1814–1832 (2012).
7. Pasindu Weerasinghe, Kate Nguyen, Priyan Mendis, Maurice Guerrieri, "Large-scale experiment on the behaviour of concrete flat slabs subjected to standard fire" Journal of Building Engineering 30 (2020) 101255.
8. Holly Kate McLeod Smith: Punching Shear of Flat Reinforced-Concrete Slabs Under Fire Conditions, Doctor of Philosophy, © 2016.
9. P. Bamonte, R. Felicetti, P.G. Gambarova, "Punching Shear in Fire damaged Reinforced Concrete Slabs, ACI Special Publication", SP265-16, (2009), pp. 345–366.
10. ISO834-1, "Fire-resistance Tests - Elements of Building Construction - Part 1: General Requirements, International Organization for Standardization", CH-1211 Gen eve 20, Switzerland, (1999). ISO834–1.
11. ASTM E119, "Standard Test Methods for Fire Tests of Building Construction and Materials", ASTM International, West Conshohocken, PA, (2000). An American National Standard, 21 pages.
12. E. Annerel, et al., "Thermo-mechanical analysis of an underground car park structure exposed to fire", Fire Saf. J. 57 (2013) 96–106.
13. P. Bamonte, R. Felicetti, "Fire scenario and structural behavior of underground parking lots exposed to fire", in: F. Wald, P. Kallerova, J. Chlouba (Eds.), In Proceeding of International Conference Applications of Structural Fire Engineering, Session 2 Fire Modeling, Prague, 19-20 February (2009), pp. 60–65.
14. ASCE, "Structural Fire Protection, ASCE Committee on Fire Protection, Structural Division, American Society of Civil Engineers", New York, (1992). Manual No. 78.
15. X.F. Hu, T.T. Lie, G.M. Polomark, J.W. MacLaurin, "Thermal Properties of Building Materials at Elevated Temperatures, Institute for Research in Construction", Canada,(1993). Internal Report No. 643, 54 pp.
16. EN1992-1-2, Eurocode2: "Design of Concrete Structures - Part 1-2: General Rules -Structural Fire Design", CEN, Brussels, (2004).
17. V. Kodur, "Properties of Concrete at Elevated Temperatures, Hindawi Publishing Corporation", ISRN Civil Engineering, (2014), pp. 1–15.
18. G.C. Thomas, A.H. Buchanan, C.M. Fleischmann, "Structural fire design: the role of time equivalence, in: Y. Hasemi (Ed.), International Association for Fire Safety Science, 5th International Symposium", Melbourne, (1997), pp. 607–618.
19. T.Z. Harmathy, "Thermal properties of concrete at elevated temperatures", J. Mater. JMLSA 5 (1) (March 1970) 47–74.
20. ACI 122R-02, "Guide to Thermal Properties of Concrete and Masonry Systems American Concrete Institute", ACI 122, Farmington Hills, MI, (2002).
21. ACI216R-89, "Guide for Determining the Fire Endurance of Concrete Elements, American Concrete Institute", ACI 216, Farmington Hills, MI, (1994). Reapproved.
22. M. Bastami, F. Aslani, E. Omran, "High-temperature mechanical properties of concrete", Int. J. Civ. Eng. 8 (4) (2010) 337–351.
23. D.J. Naus, "A Compilation of Elevated Temperature Concrete Material Property Data and Information for Use in Assessments of Nuclear Power Plant Reinforced Concrete Structures, Office of Nuclear Regulatory Research, U.S. National Nuclear Regulatory Commission", Washington, DC, (2010). NUREG/CR-7031.
24. L.Y. Li, J. Purkiss," Stress - strain constitutive equations of concrete material at elevated temperatures", Fire Saf. J. 40 (7) (2005) 669–686.
25. K. Willam, Y. Xi, K. Lee, B. Kim, "Thermal Response of Reinforced Concrete Structures in Nuclear Power Plants", Department of Civil, Environmental, and Architectural Engineering, College of Engineering, University of Colorado at Boulder, (2009). SESM No. 02.
26. D.J. Naus, "The Effect of Elevated Temperature on Concrete Materials and Structures- a Literature Review", Office of Nuclear Regulatory Research, U.S.

Nuclear Regulatory Commission, Washington, DC, (2006). NUREG/CR-6900.

27. P.J. Moss, R.P. Dhakal, G. Wang, A.H. Buchanan, "The fire behavior of multi-bay, two-way reinforced concrete slabs", Eng. Struct. 30 (2008) 3566–3573. Fig. 17. Effect of compressive strength on the slabs' ultimate strength with different pre-loadings. F.H. Arna'ot et al. Fire Safety Journal 93 (2017) 39–52.